Numerical Study of Air-Borne Acoustic Field of Stepped-Plate High-Power Ultrasonic Transducers

C Campos-Pozuelo, Antoine Lavie, B Dubus, G Rodriguez-Corral, J Gallego-Juarez

© S. Hirzel Verlag · EAA
ACUSTICA · acta acustica
Vol. 84 (1998) 1042 – 1046

Numerical Study of Air-Borne Acoustic Field of Stepped-Plate High-Power Ultrasonic Transducers

C. Campos-Pozuelo, A. Lavie*, B. Dubus†, G. Rodríguez-Corral, J. A. Gallego-Juárez
Instituto de Acústica, CSIC, Serrano, 144, 28006 Madrid, Spain

Summary
A numerical-experimental study of the displacements distribution and the radiated field of various (directional and focusing) flexural plate transducers is presented. The numerical method basically consists of calculating the distribution of displacements of the transducers by the finite element method by using the code ATILA while the corresponding radiated field is calculated by the boundary element method by means of the code EQI. In this way the near and far field of the transducers is calculated as well as their directivity pattern and vibration distribution. The obtained results are compared with experimental data. The good agreement obtained indicates that the numerical method used in this paper is a very useful tool for calculating the field of transducers and for the optimisation of their design.

PACS no. 43.35.Yb, 43.35.Zc

1. Introduction

The use of high power ultrasonics in industrial processing has increased during the last few years. Nevertheless there are many processes in which the possibilities of using ultrasonic energy have not been completely developed. In particular the application of ultrasonic waves in gases and in multiphase media (gas-liquid, gas-solid) has been limited by the lack of sufficiently effective and powerful transducers, despite industrial potentialities of using high power ultrasonics in aerosol particle precipitation, defoaming, drying, etc... [1]. The main problems for successful application to industrial processes are related with obtaining an efficient transmission of energy and improving the design and calculation methods to scale up the devices. During several years some of the authors of this paper have been involved in the development of a new type of transducer for gas-borne ultrasound which has demonstrated to be very efficient [2, 3]. The basic structure of the new transducer is shown in Figure 1. As can be seen, it consists essentially of an extensive circular plate of stepped shape driven at its centre by a piezoelectrically activated vibrator. The vibrator itself consists of a piezoelectric element of transduction in a sandwich configuration and a solid horn, which acts as a vibration amplifier. The longitudinal vibration, generated by the transducer element and amplified by the mechanical amplifier, drives the radiating plate which vibrates flexurally in its axisymmetrical modes. The elements of the transducer are calculated to be resonant at the working frequency. The extensive surface of the plate increases the radiation resistance and offers the vibrating system good impedance matching with the medium.

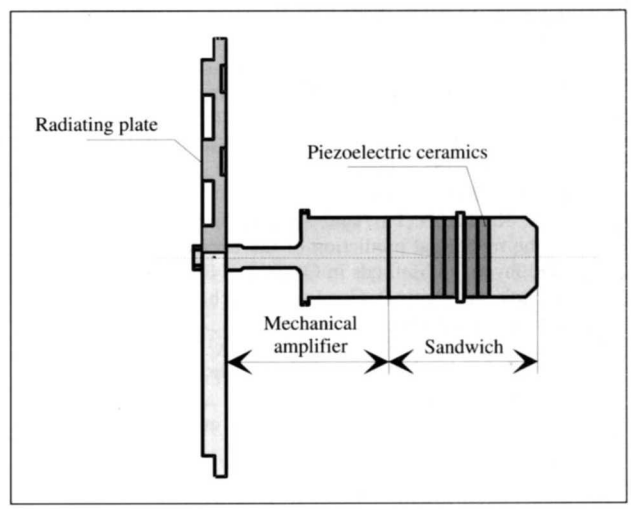

Figure 1. Scheme of the transducer.

The special profile of the plate permits the control of the vibration amplitude and the radiation pattern in such a way that high directional or focused radiation can be obtained in order to produce high-intensity acoustic levels. In fact, a flat plate radiator vibrating in its flexural modes presents in general a poor directivity due to phase cancellation. Nevertheless, if the surface elements, vibrating in counterphase on the two sides of the nodal circles, are alternately shifted along the acoustic axis direction by a quantity equal to half a wavelength, the radiation produced will be in phase across the whole beam [4] (diagrams A_0, A_1, A_2, A_3 in Figure 2) and a directivity pattern equivalent to that of the theoretical piston will be obtained. Following the same procedure it is possible, with adequate displacements of the different plate zones, to achieve any acoustic field configuration. In Figure 3 we can see, for example, the scheme of the procedure to follow for the design of a focused radiator [5]. With the same radiating-element it is possible to obtain two different configurations of the acoustic field, in correspondence with the different profile of each one of the surfaces of it.

Received 1 January 1997,
accepted 17 April 1998.

* Laboratoire d'Artois, Mécanique et Habitat, Université d'Artois, Technoparc Futura, 62400 Béthune, France

† Institut d'Electronique et de Microélectronique du Nord, département ISEN, UMR CNRS 9929, 41 boulevard Vauban, 59046 Lille Cedex, France

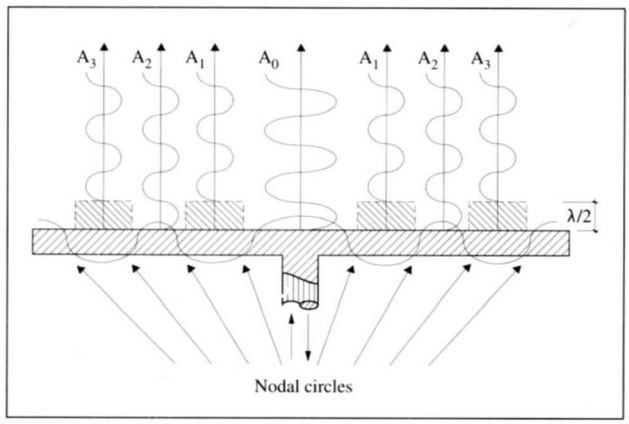

Figure 2. Scheme of the radiation mechanism for the stepped plate.

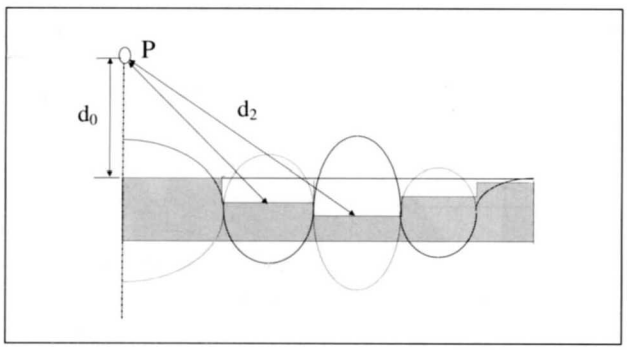

Figure 3. Scheme for the design of focusing radiators.

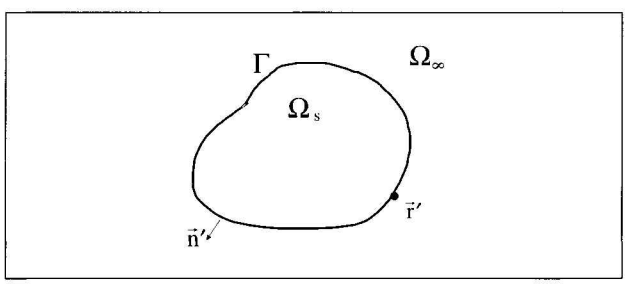

Figure 4. Domain definition.

Stepped-plate directional and focusing transducers were designed and constructed in the frequency range 10–40 kHz. The general performances obtained can be summarised as follows:

- Electroacoustic efficiency 75–80%
- Directivity (3 dB beamwidth) < 2%
- Maximum radiated levels 165 dB
- Maximum power capacity 1 kW
- Bandwidth 3–6 Hz

The procedure employed in the design of these transducers followed an analytical approach based on the Rayleigh-Ritz method [4, 6]. The radiated acoustic field was experimentally studied.

Recently, we have applied numerical methods (FEM and BEM) to simulate the transducers and to study the radiated field. In this paper we present a numerical study of the radiated field of directional and focusing stepped-plate transducers and its experimental validation. The numerical model is based on the joined application of finite element and boundary element methods. The procedure essentially consists of calculating by the finite-element method (FEM) the distribution of displacements of the transducers considering the fluid load effect obtained by the boundary element method (BEM). Then the corresponding radiated field is calculated. In this way the near and far fields of the transducers are computed as well as their directivity patterns. Some numerical and experimental data are compared in order to validate the numerical procedure.

2. Numerical evaluation

The numerical method basically consists of calculating the transducer vibration by FEM and the radiated field by BEM. The influence of the surrounding fluid is taken into account by calculating the loading impedance by BEM.

Let us consider a solid vibrating structure piezoelectrically activated Ω_s surrounded by an infinite fluid medium Ω_∞ (Figure 4). The limiting surface between Ω_s and Ω_∞ is denoted by Γ and $\boldsymbol{n}'$ (unit vector normal at each point on it) points outwards. The problem is formulated by applying FEM (ATILA code [7]) in Ω_s and BEM (EQI code [8, 9]) in Ω_∞.

2.1. Finite element method (FEM)

For the vibrating structure, the finite element set of equations is [8]:

$$\begin{bmatrix} [K_{uu}] - \omega^2[M] & [K_{u\phi}] \\ [K_{u\phi}]^T & [K_{\phi\phi}] \end{bmatrix} \begin{bmatrix} \boldsymbol{U} \\ \Phi \end{bmatrix} = \begin{bmatrix} \boldsymbol{F} \\ -\boldsymbol{q} \end{bmatrix}, \tag{1}$$

where $\boldsymbol{U}$, Φ, $\boldsymbol{q}$ and $\boldsymbol{F}$ are vectors containing the nodal values of, respectively, the mechanical displacement, the electrical potential, the electrical charges and the applied forces. $[K_{uu}]$, $[M]$, $[K_{u\phi}]$, $[K_{\phi\phi}]$ are respectively the structure stiffness, consistent mass, piezoelectric and dielectric matrices and ω is the angular frequency. $\boldsymbol{F}$ is related to the nodal pressures on Γ by the equation:

$$\boldsymbol{F} = -[L]\boldsymbol{P}, \tag{2}$$

where $[L]$ is a connectivity matrix which represents the coupling between the structure and the fluid on Γ, and $\boldsymbol{P}$ a vector containing the nodal values of the total pressure field on Γ.

The prescribed potential Φ_0 connected to one electrode (Q_0 charge) can be separated from the other potential (zero charge) and leads to the following set of equations

$$\begin{bmatrix} [K_{uu}] - \omega^2[M] & [K_{u\phi}] & [K_{u\phi_0}] \\ [K_{u\phi}]^T & [K_{\phi\phi}] & [K_{\phi\phi_0}] \\ [K_{u\phi_0}]^T & [K_{\phi\phi_0}]^T & [K_{\phi_0\phi_0}] \end{bmatrix} \cdot \begin{bmatrix} \boldsymbol{U} \\ \Phi \\ \Phi_0 \end{bmatrix} = \begin{bmatrix} -[L]\boldsymbol{P} \\ 0 \\ -Q_0 \end{bmatrix}. \tag{3}$$

ACUSTICA · acta acustica
Vol. 84 (1998)

2.2. Boundary element method (BEM)

The fluid medium is described by using the well-known Helmholtz integral formulation [10] for radiation problems

$$\iint_{\Gamma}\left[p(\boldsymbol{r}')\frac{\partial}{\partial n'}g(\boldsymbol{r}-\boldsymbol{r}')-g(\boldsymbol{r}-\boldsymbol{r}')\frac{\partial}{\partial n'}p(\boldsymbol{r}')\right]\mathrm{d}\boldsymbol{r}' = \begin{cases} p(\boldsymbol{r}) & \boldsymbol{r}\in\Omega_\infty, \\ \dfrac{\alpha(\boldsymbol{r}')}{4\pi}p(\boldsymbol{r}) & \boldsymbol{r}\in\Gamma, \end{cases} \tag{4}$$

where $\boldsymbol{r}$ is the location of the calculation point in Ω_∞ or on Γ, $\boldsymbol{r}'$ is the integration point on Γ, g is the free-space Green function, α is the solid angle formed by Γ at $\boldsymbol{r}$, $\partial/\partial n'$ denotes the outgoing normal derivative compared to $\boldsymbol{r}'$ and $\mathrm{d}\boldsymbol{r}'$ is the surface integration element. The discretisation of equation (4) on Γ leads to the following matrix equation [9]

$$[A]\boldsymbol{P} = [B]\frac{\partial p}{\partial n} = \rho_f\omega^2[B]\boldsymbol{U}_n, \tag{5}$$

where ρ_f denotes the fluid density and $\boldsymbol{U}_n$ the nodal values of the normal displacement on Γ. The $[B]$ and $[A]$ matrixes come from numerical integration of the Green function and their normal derivative averaged by the interpolation functions.

The problem caused by the irregular frequencies is solved by an overdetermination technique proposed by D. S. Jones [8, 10, 11] that uses null-field equations.

2.3. Coupling FEM-BEM

This coupling was developed for the case of quadratic elements connected by nodes on both finite element and boundary element sides. It was obtained by combining equations (3) and (5). From equation (5) the variable $\boldsymbol{P}$ is identified

$$\boldsymbol{P} = \rho_f\omega^2[A]^{-1}[B]\boldsymbol{U}_n. \tag{6}$$

To solve the problem of duplicity of normal vectors on the corners of Γ due to the discretization by quadratic elements, the matrix $[B]$ is projected along each direction and assembled in $[B_p]$ in the form

$$[B]\boldsymbol{U}_n = [B_p]\boldsymbol{U}_{(\Gamma)}, \tag{7}$$

where $\boldsymbol{U}_{(\Gamma)}$ contains the values of the components of the nodal displacement on Γ. After combining the first two equations in (3) with equations (5), (6) and (7), inserting $\boldsymbol{U}_{(\Gamma)}$ into $\boldsymbol{U}$, the following set of equations is obtained:

$$\begin{bmatrix} [K_{uu}]-\omega^2[M]+\rho_f\omega^2[L][A]^{-1}[B_p] & [K_{u\phi}] \\ [K_{u\phi}]^T & [K_{\phi\phi}] \end{bmatrix} \cdot \begin{bmatrix} \boldsymbol{U} \\ \Phi \end{bmatrix} = \begin{bmatrix} -[K_{u\phi_0}\Phi_0] \\ -[K_{\phi\phi_0}\Phi_0] \end{bmatrix}. \tag{8}$$

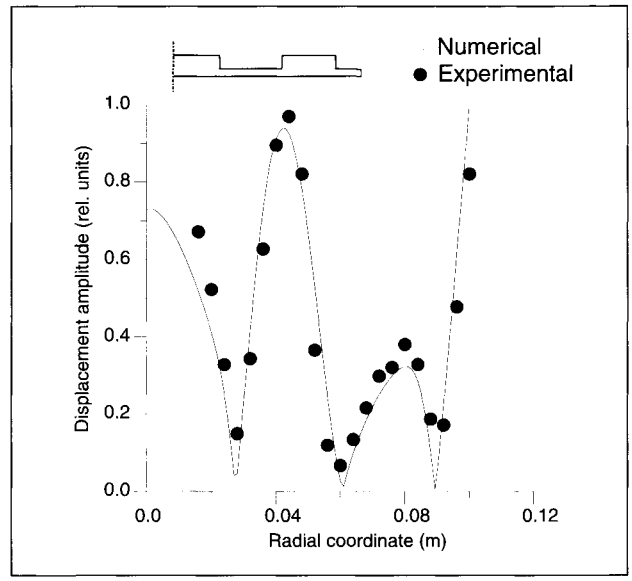

Figure 5. Distribution of displacement amplitude for a 3-nodal circle stepped-plate directional transducer. Plate radius, $r = 10\,\mathrm{cm}$, frequency, $f = 18973\,\mathrm{Hz}$.

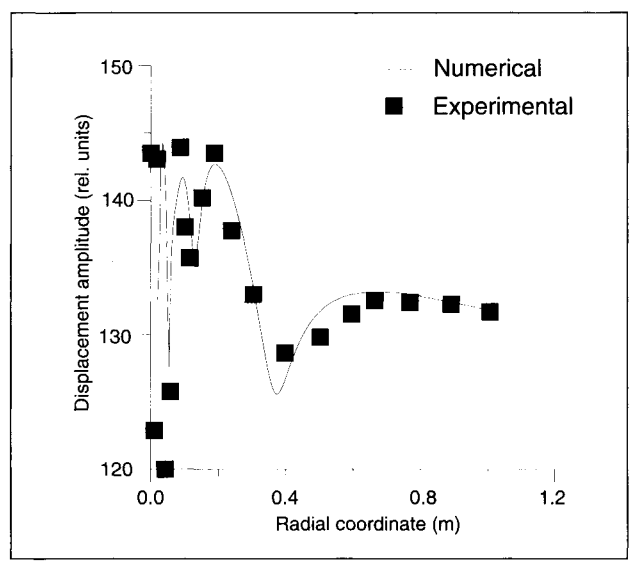

Figure 6. Sound pressure distribution along the acoustic axis for a 3-nodal circle stepped-plate directional transducer. Plate radius $r = 10\,\mathrm{cm}$, frequency $f = 18973\,\mathrm{Hz}$.

Once equations (8) are solved, the electrical impedance Z can be directly obtained from the third equation in (3),

$$Z = \frac{\Phi_0}{\mathrm{i}\omega Q_0} = \frac{\mathrm{i}\Phi_0}{\omega\left([K_{u\phi_0}]^T\boldsymbol{U}+[K_{\phi\phi_0}]^T\Phi_0+[K_{\phi_0\phi_0}]\Phi_0\right)}. \tag{9}$$

$\boldsymbol{U}_{(\Gamma)}$ will be known and used together with equations (6) and (7) will give the surface pressures. The pressure field in Ω_∞ is then obtained from equation (4). This coupling procedure was implemented in the ATILA and EQI codes for axisymmetrical and tridimensional analyses.

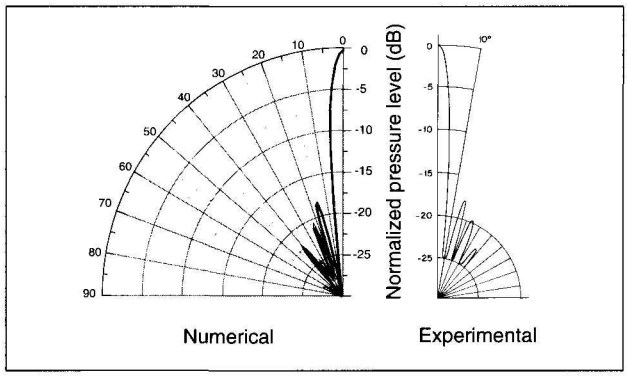

Figure 7. Numerical-experimental comparison of the directivity pattern for a 3-nodal circle stepped-plate directional transducer. Plate radius, $r = 10$ cm. Frequency, $f = 18973$ Hz.

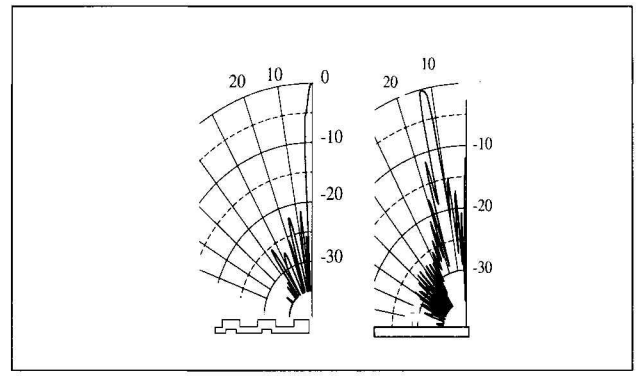

Figure 9. Comparison between computed directivities of a 5 nodal circle stepped-plate transducer and a flat-plate transducer. Plate radius $r = 16$ cm, frequency $f = 19382$ Hz.

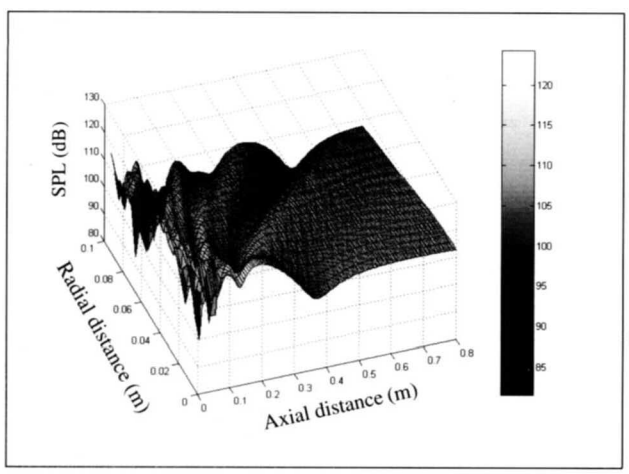

Figure 8. Computed acoustic field of a 3-nodal circle stepped-plate directional transducer Plate radius $r = 10$ cm, frequency $f = 18973$ Hz.

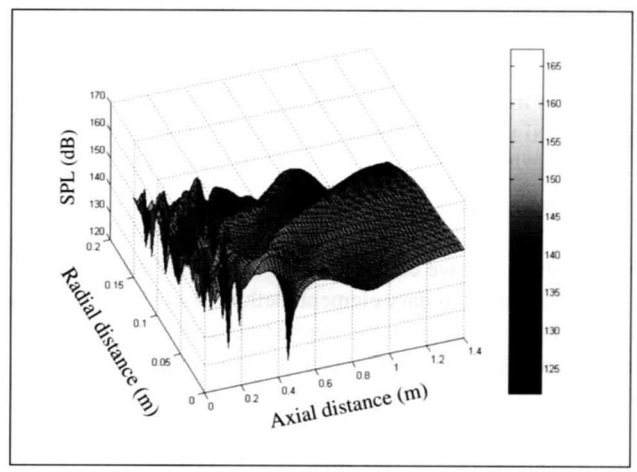

Figure 10. Computed acoustic field of a 5-nodal circle stepped-plate directional transducer. Plate radius $r = 16$ cm, frequency $f = 19382$ Hz.

3. Validation of the procedure

To validate the numerical procedure, a comparison between experimental and numerical data was made for a transducer with a stepped-plate vibrating axisymmetrically with three nodal circles. Figure 5 shows the comparison for the vibration amplitude distribution. Figure 6 shows the numerical and experimental data for the sound pressure distribution along the acoustic axis. Finally, Figure 7 shows the comparison for the directivity patterns. From these comparisons it is clear that a good agreement is obtained and therefore the validity of the procedure is demonstrated. To be noted the high-directional piston-like radiation obtained from this kind of transducers. The non-uniform distribution of displacement amplitude that we observe in Figure 5 causes some differences between the lateral lobes of the radiation from a flexural stepped-plate transducer and that from an ideal piston. Nevertheless, we can see (Figure 7) that the level of these lateral lobes is of the order of 20 dB smaller than the level of the main lobe. Therefore the lateral lobes have a small incidence in the whole radiation.

4. Application of the numerical procedure to the study of stepped-plate transducers

We applied the numerical procedure to the study of the vibrational behaviour and the radiation characteristics of several directional and focused transducers. Figure 8 shows the acoustic field of the previous 3-nodal circle stepped-plate directional transducer. As it can be seen by using this procedure we have the full map of the acoustic field which is very difficult to obtain experimentally.

By following the same procedure we compare the directivity pattern for a 5-nodal circle stepped-plate directional transducer with a flat-plate transducer of the same plate diameter (Figure 9). The directional effect of the stepped-plate radiator is very clear. Figure 10 shows the full acoustic field of the same transducer.

Finally the results obtained for focused transducers are shown. In Figure 11 the full acoustic field for a 5-nodal circle stepped-plate is displayed. Figure 12 shows the axial pressure distribution, and the radial pressure distribution at the central plane of the focus for a 7-nodal circles stepped-plate focused transducer. To be noted that the focus obtained

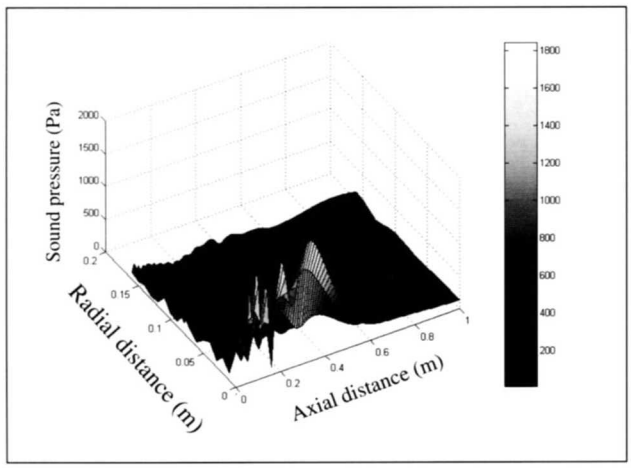

Figure 11. Computed acoustic field of a 5-nodal circle stepped-plate focused transducer. Plate radius, $r = 16$ cm. Frequency, $f = 19382$ Hz.

with this transducer (measured at 3 dB) corresponds to an ellipsoidal volume of about 16 cm and 2 cm in diameters.

5. Conclusions

As a conclusion we can assure the validity of the combined finite element-boundary element methods as an excellent tool to improve the design of the stepped-plate transducer, to have a full knowledge of their characteristics and to analyse the influence of the plate profile in the radiated acoustic field.

In addition, this new procedure greatly facilitates to scale the transducers up to very high power capacities. As an example, it is to be mentioned the present development of a transducer with a plate of one meter in diameter and an estimated power capacity of about 3 kilowatts.

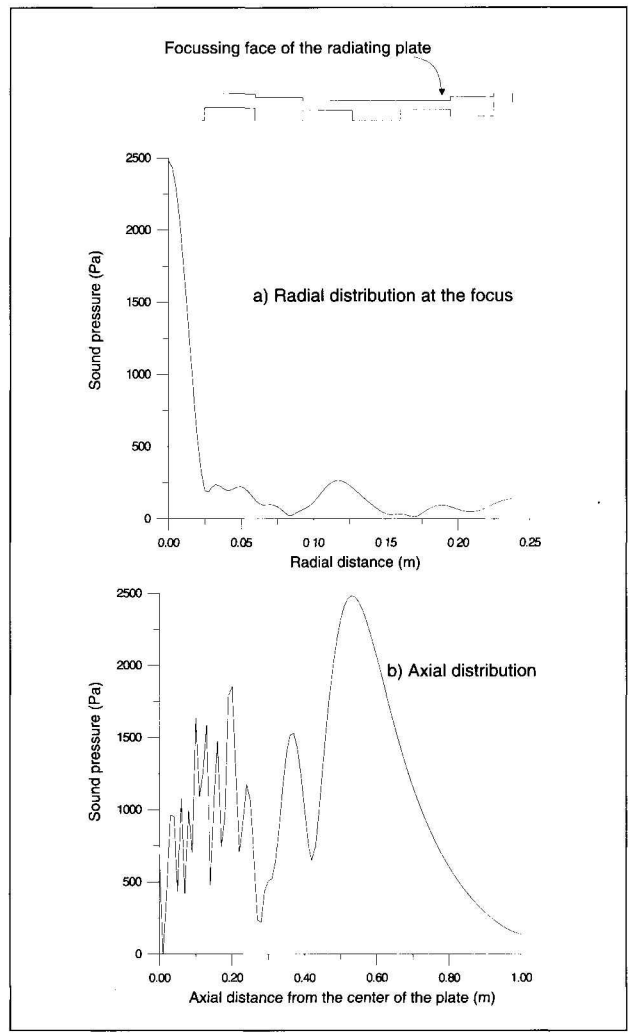

Figure 12. Computed sound pressure distributions for a 7-nodal circle stepped-plate focused transducer.

Acknowledgement

This research was supported by a postdoctoral fellowship of the DGICT (State Secretary of Universities and Research) Ref: EX94 70735053 and a Post-Doctoral Contract of the CSIC (Higher Council for Scientific Researchs).The work was developed within the frame of the Projects CICYT-AMB96-A211-CO2 and BRITE/EURAM BRPR-CT96-0157.

References

J. A. Gallego-Juárez: Transducer needs for macrosonics. – In: Power transducers for sonics and ultrasonics. B. Hamonic, J. N. Decarpigny (eds.). Springer-Verlag, Berlin, 1990, 35–47.

J. A. Gallego-Juárez: High power ultrasonic transducers for use in gases and interphases. – In: Power Sonic and Ultrasonic Transducers Design. B. Hamonic, J. N. Decarpigny (eds.). Springer-Verlag, Berlin, 1988, 175–184.

J. A. Gallego-Juárez, G. Rodríguez-Corral, L. Gaete-Garretón: An ultrasonic transducer or high power applications in gases. Ultrasonics **16** (1978) 267–271.

A. Barone, J. A. Gallego-Juárez: Flexural vibrating free-edge plates with stepped thicknesses or generating high directional ultrasonic radiation. J. Acoust. Soc. Am. **51** 953–959.

G. Rodríguez-Corral, J. L. San Emeterio, J. A. Gallego-Juárez: Focused high-power ultrasonic transducer with stepped-plate radiator for industrial application in gases. Ultrasonic International 87 Conference Proceedings, 1987. 794–797.

J. L. San Emeterio, J. A. Gallego-Juárez, G. Rodríguez-Corral: High axisymmetric modes of vibration of stepped circular plates. J. Sound Vib. **114** (1987) 495–505.

J.-N. Decarpigny, J.-C. Debus, B. Tocquet, D. Boucher: In-air analysis of piezoelectric Tonpilz transducers in a wide frequency band using a mixed finite element-plane wave method. J. Acoust. Soc. Am. **78** (1985) 1499–1507.

B. Stupfel, A. Lavie, J.-N. Decarpigny: Combined integral equation formulation and null-field method for the exterior acoustic problem. J. Acoust. Soc. Am. **83** (1988) 927–941.

A. Lavie: Modelisation du rayonnement ou de la diffraction acoustique par une méthode mixte équation intégrales-champ nul. Dissertation. Lille University, 1989.

H. A. Schenck: Improved integral formulation for acoustic radiation problems. J. Acoust. Soc. Am. **44** (1967) 41–58.

D. S. Jones: Integral equations for the exterior acoustic problem. Q. J. Mech. Appl. Math. **XXVII** (1973) 129–142.